

## Ultrasonic Treatment of Polyacrylic Acid Sodium/NaA Zeolite Hybrid Membranes for the Pervaporation Dehydration of Ethanol

Ping Wei,<sup>1</sup> Xin Ying Qu,<sup>1</sup> Hang Dong,<sup>1</sup> Lin Zhang,<sup>1</sup> Huanlin Chen,<sup>1</sup> Congjie Gao<sup>1,2</sup>

<sup>1</sup>Department of Chemical & Biological Engineering, Engineering Research Center of Membrane & Water Treatment Technology, MOE, Zhejiang University, Hangzhou 310027, People's Republic of China

<sup>2</sup>The Development Center of Water Treatment Technology, Hangzhou 310012, People's Republic of China

Correspondence to: L. Zhang (E-mail: linzhang@zju.edu.cn)

**ABSTRACT:** Ultrasonics was used to improve the dispersion of NaA zeolite in polyacrylic acid sodium (PAAS) membranes. The effect of ultrasonication time on the dispersion of NaA zeolite in the membranes, the membrane structure, and performance were investigated. The casting solution and resulting membranes were characterized by viscosity measurement, polarizing optical microscopy (POM), scanning electron microscopy, and X-ray diffraction (XRD). With increasing ultrasonication time, the viscosity of the casting solution decreased as the chain entanglements decreased. The POM and XRD results showed that crystallization occurred in the PAAS membrane after ultrasonic processing. A more homogeneous morphology was obtained due to improvement in the dispersion of zeolite under ultrasonic treatment for 0.5–1.0 h. As a result, the separation performance was enhanced. The water/ethanol separation factor increased from 176.2 to 577.8. However, the relative separation factor decreased when the ultrasonic time exceeded 2.5 h, due to the appearance of a lamellar structure. © 2013 Wiley Periodicals, Inc. *J. Appl. Polym. Sci.* 000: 000–000, 2013

**KEYWORDS:** polyacrylic acid sodium; NaA zeolite; ultrasonic treatment; crystallization; pervaporation membrane

Received 19 April 2013; accepted 19 June 2013; Published online

DOI: 10.1002/app.39685

### INTRODUCTION

The strategy of forming a hybrid membrane by dispersing inorganic fillers in a polymeric matrix has presented advantages in the development of advanced membranes for numerous separation processes, such as gas separation and pervaporation.<sup>1–4</sup> However, it has been found that there is an obstacle to the successful introduction of inorganic porous materials into an organic polymer matrix due to the incompatibility between the porous particles and polymer matrix. In addition, inorganic porous materials often agglomerate. Various techniques exist for the dispersion of particle agglomerates, such as the application of high shear forces during mechanical stirring<sup>5</sup> and the direct incorporation by chemical methods.<sup>6</sup> Another suitable alternative technique for the dispersion of nanoparticles is ultrasonication.<sup>7–15</sup> For instance, Boukerrou et al.<sup>8</sup> successfully incorporated titanium dioxide nanoparticles into epoxy resin via the ultrasonic process. Jun et al.<sup>10</sup> found that the dispersion and adhesion of B<sub>4</sub>C particles in epoxy resin can be enhanced by using direct ultrasonic excitation. Meanwhile numerous studies have shown that ultrasonication has an impact on the structure and crystalline order of a polymer.<sup>11–15</sup> These studies have shown that ultrasonic treatment can degrade polymer chains. The relative motion of the polymer segments and solvent molecules resulting from the ultrasound

gives rise to shear stresses on the polymer chain, leading to the scission of the polymer chain.<sup>16</sup> Ultrasonic treatment is a simple method to improve the crystalline order in polymers.<sup>17–22</sup> Khamad et al.<sup>21</sup> studied the extrusion process of HDPE containing a small amount of butyl rubber under ultrasonic irradiation and found that the crystallinity increased, the structural defects were reduced, and the mechanical properties were enhanced. Zhao et al.<sup>22</sup> studied a new method to improve poly(3-hexyl thiophene) crystalline behavior, and found that more ordered precursors were generated in solution due to an increased self-assembly from disordered to ordered conformation after ultrasonic oscillating.

The properties of the casting solutions, such as different casting solvents, viscometric behavior, and additives, can bring about different membrane structures, and this affects their separation performances.<sup>23,24</sup> Based on the above reports, it can be deduced that membrane morphology and separation performance can be altered by the ultrasonic treatment of the casting solution.

The objective of this work was to study the structure of polyacrylic acid sodium (PAAS)/NaA zeolite hybrid membranes and membrane morphology by polarizing optical microscopy (POM) and X-ray diffraction (XRD) techniques after the

ultrasonication of the solutions from which they were cast, and the effect of the structure of the PAAS/NaA zeolite hybrid membranes on the performance of pervaporation.

## EXPERIMENTAL

### Materials and Chemicals

PAAS (MW: 3,000,000) and ethanol were purchased from Sino-pharm Chemical Reagent, China. 3-Aminopropyltriethoxysilane was bought from Tokyo Kasei, Japan. Polyacrylonitrile ultrafiltration (PAN) membranes (MWCO: 20,000) were used as the support and were supplied by the Department Center of Water Treatment Technology, Hangzhou, China. A-type zeolite (NaA) was synthesized in our lab. Sodium aluminate ( $\text{NaAlO}_2$ , 99.9%) was purchased from Strem Chemicals. Tetrapropylammonium hydroxide ( $\text{NaSiO}_3 \cdot 9\text{H}_2\text{O}$ , 99 wt %) was bought from Aldrich. Ethanol was purchased from Sinopharm Chemical Reagent, China. Deionized water was used in all experiments.

### Synthesis of NaA Zeolite

The synthesis method has been reported previously.<sup>25</sup> The NaA zeolites were synthesized by mixing a solution with molar compositions of  $\text{Na}_2\text{O} : \text{SiO}_2 : \text{Al}_2\text{O}_3 : \text{H}_2\text{O} = 4.9 : 1.6 : 1 : 173$  in a sealed polypropylene bottle.

### Membrane Preparation

PAAS/NaA zeolite hybrid membranes and pristine PAAS membranes were fabricated by a solution-casting method. Specific amounts of NaA zeolite were distributed in the deionized water and redispersed under ultrasonication for 20 min. Afterward the PAAS was added to the NaA zeolite solution. The weight fraction of NaA zeolite in the PAAS matrix was varied from 0 to 15 wt %, and the PAAS concentration of the casting solutions was adjusted to 1.5 wt %. After stirring at room temperature for 72 h, the casting solution was ultrasonicated using ultrasonic device (KQ3200E, Kunshan, 150 W, 40 kHz) for certain lengths of time, and then homogeneous casting solutions were obtained after standing for 6 h. The solution was cast onto the PAN support membranes, which were previously fixed on glass plates, with the aid of a casting knife. The membranes were heated at 50°C for 2–3 h and then held at room temperature for 12 h, yielding the PAAS/NaA zeolite hybrid membranes. The thickness of the composite membranes was about 133  $\mu\text{m}$  including PAAS or PAAS/NaA and PAN supported membrane. Pristine PAAS membranes were fabricated in exactly the same way as above without incorporating NaA zeolite.

### Characterization

The structures of the PAAS and PAAS/NaA membranes without PAN supported membranes were studied at room temperature using a D-8 advanced wide-angle  $K_\alpha$  X-ray diffractometer (Bruker). The X-ray source was Ni-filtered  $\text{Cu } K_\alpha$  radiation (40 kV, 30 mA). The dried membranes of uniform thickness ( $40 \pm 2 \mu\text{m}$ ) without PAN supported membrane were mounted on a sample holder and the patterns were recorded in the reflection mode at an angle  $2\theta$  over a range of 5–90° at a speed of 8°/min. The morphology of the samples was observed with a Nikon Eclipse E400 polarizing optical microscope (Japan). Surface morphologies of the membranes were examined by a scanning electron microscopy (SEM) instrument (SIRION-100, FEI)

at an acceleration voltage of 25 kV, and the samples were coated with gold for 30 s.

### Viscosity Measurement

The viscosities of the casting solution subjected to different ultrasonication time were measured using a NXS-11A rotational viscometer (China) at 25°C and chose two rotation frequency which is 5.6 r/min and 7.6 r/min to obtain average viscosity.

### PV Measurements

A flat-sheet membrane including the PAN support with an effective area of 18.1  $\text{cm}^2$  was used for the evaluation of water/ethanol separation performance. The experimental procedure was reported in detail in a previous publication.<sup>26</sup> An aqueous solution of ethanol was continuously circulated from the feed tank to the upstream side of the membrane. The temperature of the feed mixture was kept constant by means of a water jacket with a thermostat at 30°C. The vacuum on the downstream side was maintained at about 135 Pa by a vacuum pump. The permeate was collected in a cold trap. The compositions of the permeate and the feed were determined on a gas chromatograph (GC-950, China) equipped with a 2.0-m long column packed with Porapak Q and a TCD detector with the column temperature set at 120°C. From the collection amount and permeation product composition, the permeation flux and separation factor can be obtained by the following equations:

$$J = \frac{\Delta g}{S \times \Delta t} \quad (1)$$

$$\alpha = \frac{P_{\text{ethanol}} / P_{\text{water}}}{F_{\text{ethanol}} / F_{\text{water}}} \quad (2)$$

where  $\Delta g$  is the permeation weight collected in the cold traps during operation time  $\Delta t$ ;  $S$  is the membrane area (18.1  $\text{cm}^2$ );  $F_{\text{ethanol}}$  and  $F_{\text{water}}$  are the weight fractions of ethanol and water in the feed;  $P_{\text{ethanol}}$  and  $P_{\text{water}}$  are the weight fractions in the permeate, respectively.

## RESULTS AND DISCUSSION

### Viscosity of the Casting Solution with Different Ultrasonication Time

The viscosities of the membrane casting solutions with different ultrasonication time are listed in Table I. When zeolite was added the viscosity of the casting solution increased from 2499 to 3233  $\text{mPa} \cdot \text{s}$  for an untreated solution containing 10 wt % of NaA zeolite. A similar phenomenon has been reported by Bittmann et al.<sup>27</sup> They found that adding  $\text{TiO}_2$  nanoparticles in epoxy resin caused a strong increase in viscosity up to 8  $\text{Pa} \cdot \text{s}$  for RM 300 and up to 10  $\text{Pa} \cdot \text{s}$  for RM 400, from 0.02  $\text{Pa} \cdot \text{s}$ . We speculated that the negatively charged carboxyls of PAAS bonded with  $\text{Na}^+$  in the NaA zeolite strongly and thus formed a local supersaturation microenvironment. Moreover, the strong electric field resulting from the high concentration of negatively charged carboxyls favored the interaction with the positively charged NaA zeolite. Therefore, the casting solution formed a gel when NaA zeolite was incorporated,<sup>28–30</sup> and the viscosity of the casting solution increased.

However, for the 10 wt % zeolite-loaded PAAS casting solution, the viscosity decreased sharply after ultrasonic treatment.

**Table I.** The Viscosity of the Membranes Casting Solutions Subjected to Different Ultrasonication Time

Membrane casting solution	Ultrasonication time (h)	Viscosity (mPa · s)
Pure PAAS	0	2499
	0.5	1499.4
	1.0	739.2
	1.5	369.6
	2.5	95.3
NaA-PAAS <sup>a</sup>	0	3233
	0.5	1809
	1.0	625.7
	1.5	257.8
	2.5	59.2
	3.5	50.9

<sup>a</sup>The mass ratio of zeolite to PAAS was 10 wt %.

When the ultrasonic time increased from 0.5 to 1.5 h, the viscosity of the casting solution decreased from 1809 to 257.8 mPa · s. When the ultrasonic time exceeded 2.5 h, the viscosity of the casting solution was less than 100 mPa · s. It is due to the fact that degradation of the PAAS resulted from cavitations that were formed when ultrasound waves of sufficient intensity propagated through the solution. Intense shear

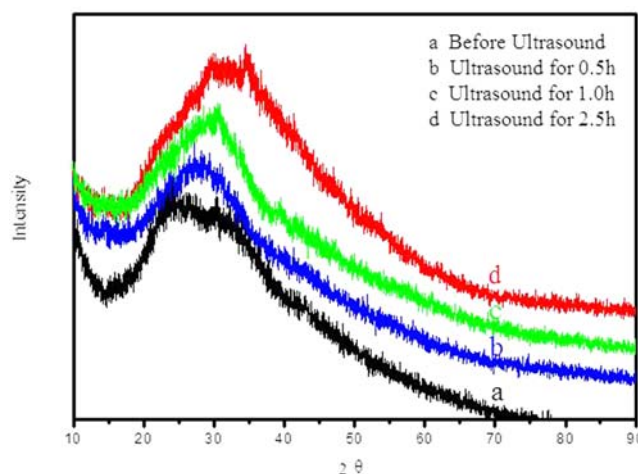


**Figure 1.** The XRD of PAAS membrane with the casting solution ultrasonicated for (a) 0 h (b) 0.5 h, (c) 1.0 h, and (d) 2.5 h. [Color figure can be viewed in the online issue, which is available at [wileyonlinelibrary.com](http://wileyonlinelibrary.com).]

fields were generated during the collapse of the microbubbles, and the PAAS segments near the collapsing cavity moved faster than those farther away from the collapsing cavity. This relative motion of the polymer segments and solvent molecules gave rise to shear stresses in the polymer chain leading to scission.<sup>31</sup> Thus the viscosity of the polymer decreased after ultrasonication.

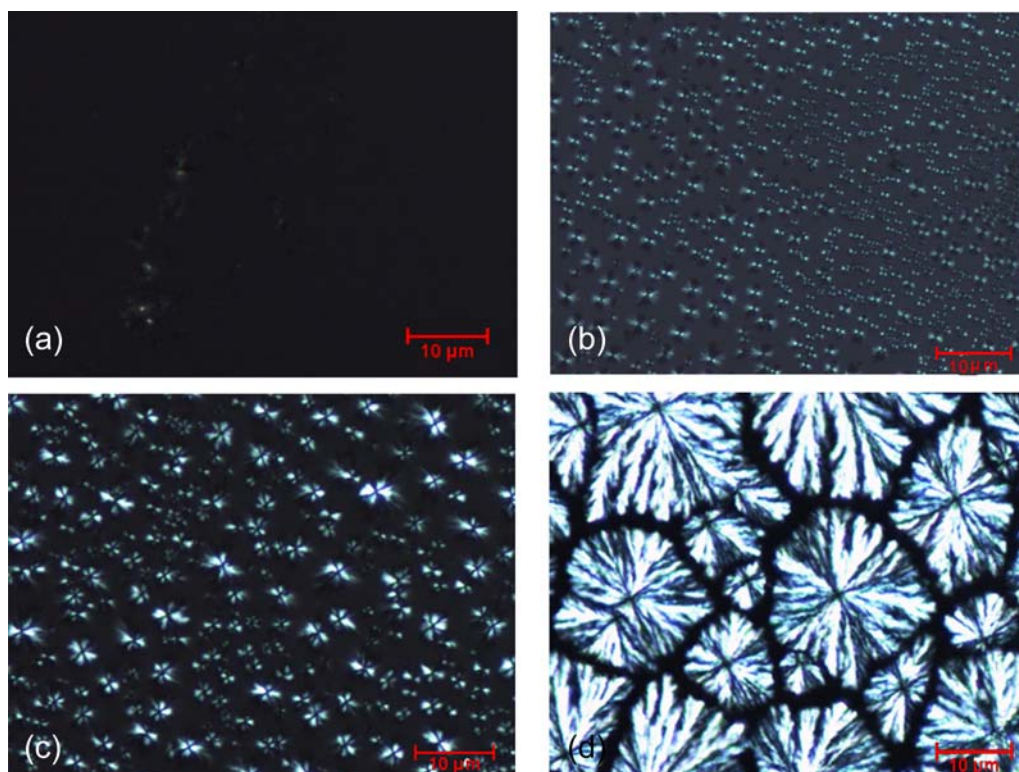


**Figure 2.** Polarizing microscopy image of PAAS membranes with the casting solution subjected to different ultrasonication time (a) 0 h, (b) 0.5 h, (c) 1.0 h, and (d) 2.5 h. [Color figure can be viewed in the online issue, which is available at [wileyonlinelibrary.com](http://wileyonlinelibrary.com).]

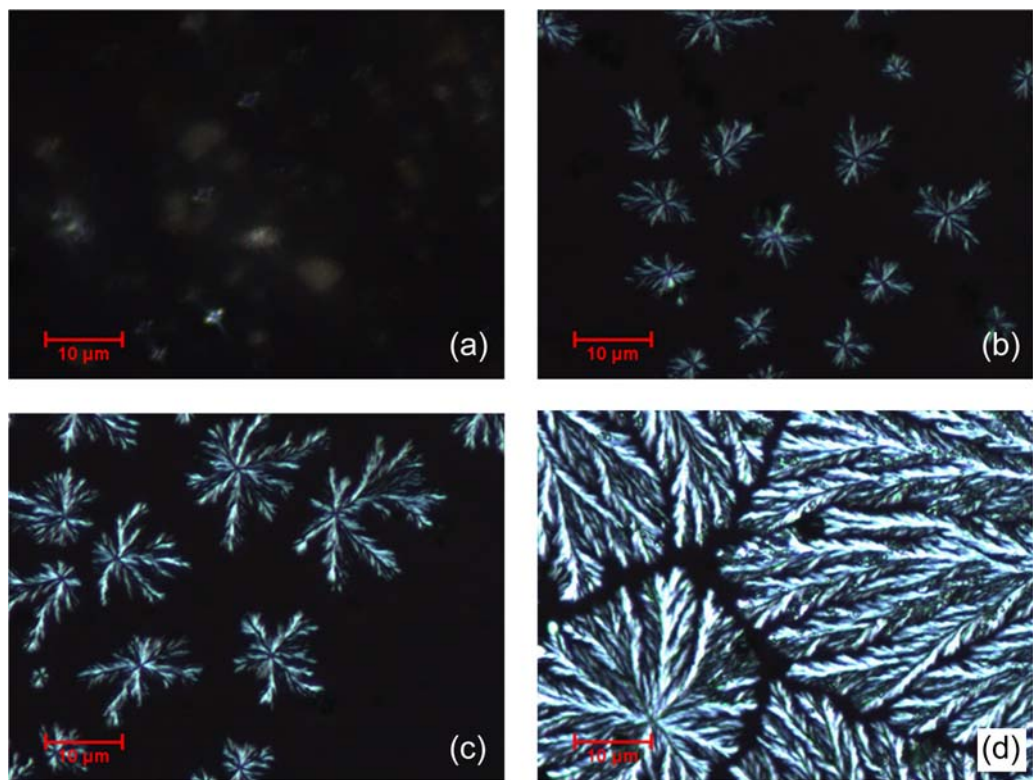


**Figure 3.** Polarizing microscopy image of PAAS/NaA hybrid membranes with 10 wt % NaA with the casting solution subjected to different ultrasonication time (a) 0 h, (b) 0.5 h, (c) 1.0 h, and (d) 2.5 h. [Color figure can be viewed in the online issue, which is available at [wileyonlinelibrary.com](http://wileyonlinelibrary.com).]

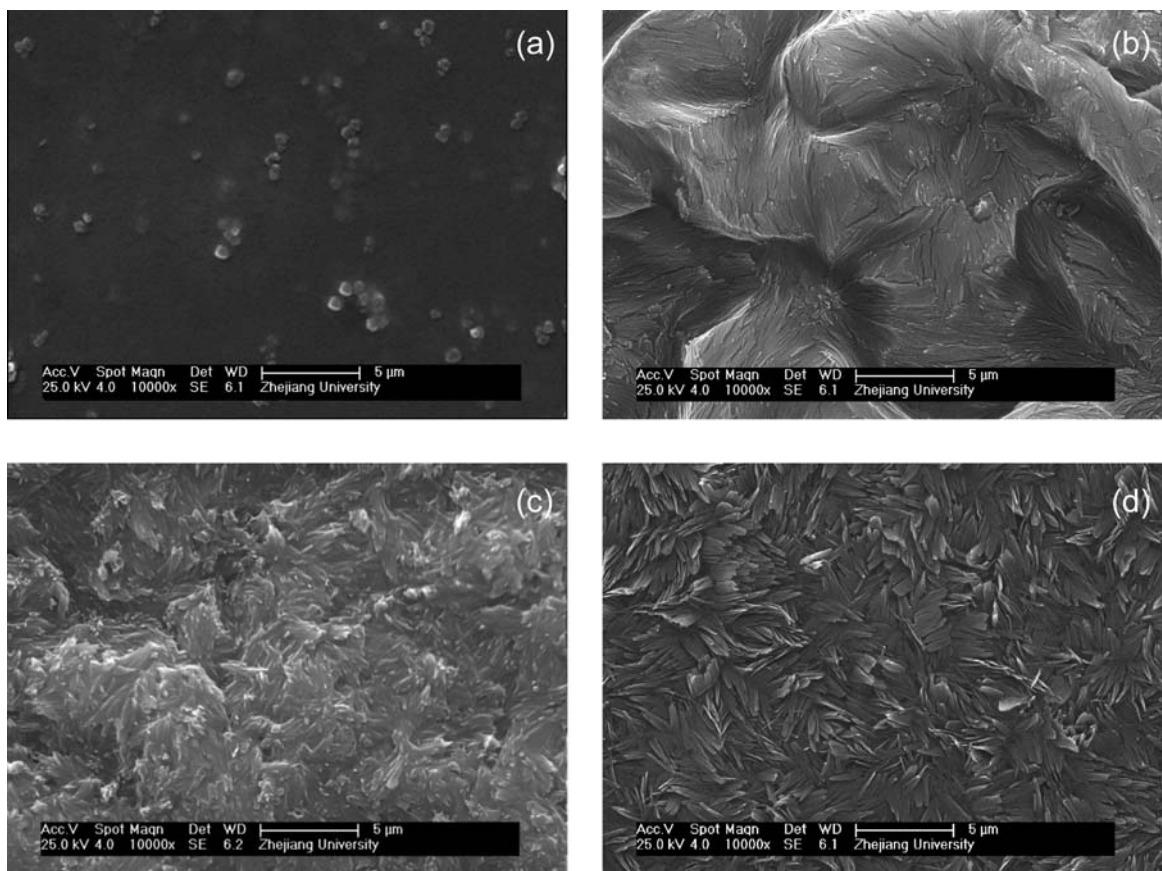


**Figure 4.** Surface SEM micrographs of 10 wt % modified zeolite filled hybrid membrane with the casting solution subjected to different ultrasonication time (a) 0 h, (b) 0.5 h, (c) 1.0 h, and (d) 2.5 h.

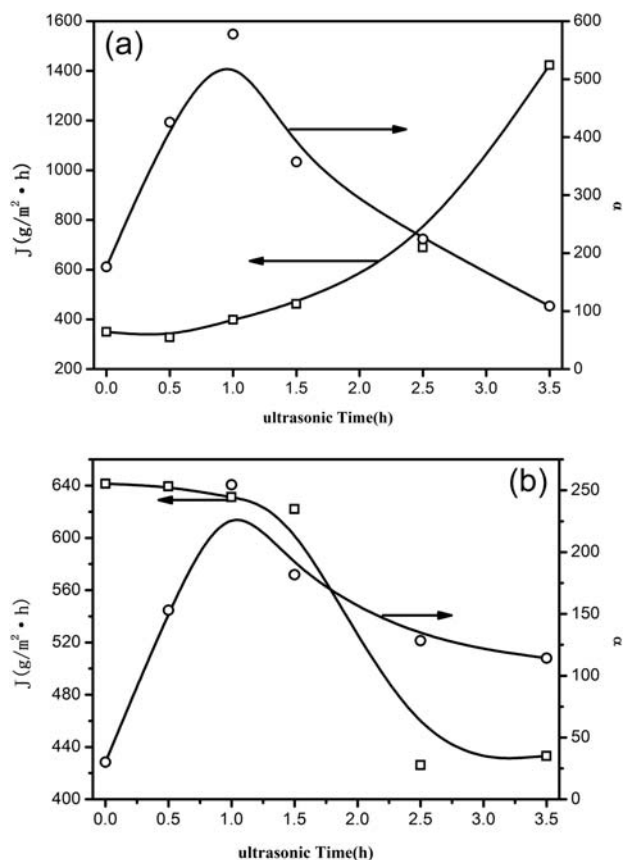


**Figure 5.** Effect of ultrasonication time of the casting solution on the pervaporation performance of 10 wt % modified NaA zeolite loaded hybrid membranes (a) and the pure PAAS (b) for dehydration of 90 wt % ethanol aqueous solution at operation temperature of 30°C.

### XRD and POM of PAAS and PAAS/NaA Zeolite Hybrid Membranes

Figure 1 shows the XRD patterns of the PAAS membrane without PAN supported membrane. The bare PAAS membrane has no sharp peak without ultrasound treatment. After ultrasonic treatment, a crystalline peak appeared and crystalline intensity was increased with the ultrasonic time increasing. The results indicated that the molecular structure is likely to be ordered after ultrasonic treatment. POM images of the PAAS membrane and PAAS/NaA zeolite hybrid membrane with the casting solution subjected to different ultrasonic times are shown in Figures 2 and 3. Before ultrasonic treatment there were no crystals. The crystals grew larger with increasing ultrasonication time. The trend was similar for both the PAAS and PAAS/NaA zeolite hybrid membranes. Furthermore, the crystals in the hybrid membrane were larger than in the PAAS membrane. This phenomena can be explained by the following reasons. First ultrasonication led to scission and the short chains of polymer drove the packing and long-range ordering of the chains. Meanwhile, the zeolite could act as a nucleus to which more chains aggregate. As a result, more crystals grew from the central nucleus.

### Membrane Morphology

In this study, the casting solution with 10 wt% modified NaA zeolite loaded was ultrasonicated for different periods of time.

The surface morphology of the resulting hybrid membranes were imaged by SEM. As shown in Figure 4, when the ultrasonication time was not too long, the membrane morphology was more homogenous. From the above discussion about viscosity, the proper viscosity was obtained when the ultrasonic time lay between 1.0 and 1.5 h, which is beneficial to the dispersion of zeolite in the PAAS matrix.<sup>27</sup> However, the membrane morphology became rough and formed a lamellar morphology when the casting solution was ultrasonicated for 2.5 h.

### Effect of Ultrasonication Time on Pervaporation Performance

The effects of ultrasonication time on the pervaporation performance of the pure PAAS and 10 wt % NaA zeolite loaded hybrid membranes are shown in Figure 5. With increasing ultrasonication time, the permeation flux increased sharply but the separation factor first increased then decreased for the hybrid membrane. This is due to the membrane morphology becoming more homogenous when the casting solution was ultrasonicated for 0.5–1.0 h. Therefore, the separation factor increased. However, when the ultrasonication time exceeded 1.5 h, the crystallinity of the membrane increased sharply and the membrane morphology formed a lamellar structure. Therefore, as shown in Figure 5(a), the permeation flux increased significantly; however, the separation factor first increased then decreased. The change in flux of the pure PAAS membranes were opposite to that of the hybrid membranes, as shown in Figure 5(b), the reason could be that the crystallinity of the membrane increased with increasing ultrasonic time due to the polymer segments becoming more ordered and dense. The dense segments of polymer are barriers that reduced the space available for diffusion.

### CONCLUSION

Ultrasonic treatment was used to improve the dispersion of zeolite in a hybrid membrane. Crystals formed with increasing ultrasonic time. The membrane performance changed caused by the crystalline structure. The water/ethanol separation factor first increased from 176.2 to 577.8 with ultrasonic time of 0.5–1.0 h. However, a lamellar structure appeared clearly when the ultrasonic time exceeded 2.5 h, and the relative separation factor decreased. Combined the results of flux, the optimum ultrasonic time is 1.0 h for PAAS and PAAS/NaA zeolite membranes.

### ACKNOWLEDGEMENTS

This project was sponsored by the National Hi-Tech Research and Development Program of China (2009AA02Z208), the National Basic Research Program of China (2009CB623402), and the Fundamental Research Funds for the Central Universities of China.

### REFERENCES

1. Tan, H. F.; Wu, Y. H.; Li, T. M. *J. Appl. Polym. Sci.* **2013**, *129*, 105.
2. Prasad, C. V.; Swamy, B. Y.; Sudhakar, H.; Sobharani, T.; Sudhakar, K.; Subha, M. C. S.; Rao, K. C. *J. Appl. Polym. Sci.* **2011**, *121*, 1521.
3. Qiu, S.; Wu, L. G.; Shi, G. Z.; Zhang, L.; Chen, H. L.; Gao, C. *J. Ind. Eng. Chem. Res.* **2010**, *49*, 11667.

4. Gomes, D.; Nunes, S. P.; Peinemann, K. V. *J. Membr. Sci.* **2005**, *246*, 13.
5. Wetzel, B.; Hauptert, F.; Zhang, M. Q. *Compos. Sci. Technol.* **2003**, *63*, 2055.
6. Kang, S.; Hong, S. I.; Choe, C. R.; Park, M.; Rim, S.; Kim, J. *Polymer* **2001**, *42*, 879.
7. Xu, L. R.; Bhamidipati, V.; Zhong, W. H.; Li, J.; Lukehart, C. M.; Lara-Curzio, E.; Liu, K. C.; Lance, M. J. *J. Compos. Mater.* **2004**, *38*, 1563.
8. Boukerrou, A.; Duchet, J.; Fellahi, S.; Sautereau, H. *J. Appl. Polym. Sci.* **2007**, *105*, 1420.
9. Bittmann, B.; Hauptert, F.; Schlarb, A. K. *Ultrason. Sonochem.* **2009**, *16*, 622.
10. Jun, J.; Kim, J.; Bae, Y.; Seo, Y. S. *J. Nucl. Mater.* **2011**, *416*, 293.
11. Taghizadeh, M. T.; Mehrdad, A. *Ultrason. Sonochem.* **2003**, *10*, 309.
12. Taghizadeh, M. T.; Asadpour, T. *Ultrason. Sonochem.* **2009**, *16*, 280.
13. Shukla N. B.; Darabonia, N. Madras, G. *J. Appl. Polym. Sci.* **2009**, *112*, 991.
14. Koda, S.; Mori, H.; Matsumoto, K.; Nomura, H. *Polymer* **1994**, *3*, 30.
15. Qian, J. W.; Zhou, G. H.; An, Y. L. *J. Appl. Polym. Sci.* **2001**, *81*, 2798.
16. Price, G. *J. Adv. Sonochem.* **1990**, *1*, 231.
17. Ding, Y.; Osaka, A.; Miura, Y. *J. Am. Ceram. Soc.* **1994**, *77*, 749.
18. Kang, J.; Chen, J. Y.; Cao, Y.; Li, H. L. *Polymer* **2010**, *51*, 249.
19. Liu, H.; Hu, X. B.; Wang, J. Y.; Boughton, R. I. *Macromolecules.* **2002**, *35*, 9414.
20. Cao, Y. R.; Xiang, M.; Li, H. L.; J. *Appl. Polym. Sci.* **2002**, *84*, 1956.
21. Khamad, S. I.; Popova, E. N.; Salina, Z. I. *Deposited Doc. (RUSS), VINITI* **1984**, 1829.
22. Zhao, K.; Xue, L. J.; Liu, J. G.; Gao, X.; Wu, S. P. *Langmuir* **2010**, *26*, 471.
23. Qian, J. W.; Miao, Y. M.; Zhang, L.; Chen, H. L. *J. Membr. Sci.* **2002**, *203*, 167.
24. Tsitsilianis, C.; Staikos, G.; Dondos, A. *Polymer* **1992**, *33*, 3369.
25. Wei, P.; Qu, X. Y.; Dong, H.; Zhang, L.; Chen, H. L.; Gao, C. J. *J. Appl. Polym. Sci.* **2013**, *128*, 3390.
26. Qu, X. Y.; Dong, H.; Zhou, Z. J.; Zhang, L.; Chen, H. L. *Ind. Eng. Chem. Res.* **2010**, *49*, 7504.
27. Bittmann, B.; Hauptert, F.; Schlarb, A. K. *J. Appl. Polym. Sci.* **2012**, *124*, 1906.
28. Yu, J. G.; Lei, M.; Cheng, B.; Zhao, X. J. *J. Solid State Chem.* **2004**, *177*, 681.
29. Yua, J. G.; Lei, M.; Cheng, B.; Zhao, X. J. *J. Cryst. Growth* **2004**, *261*, 566.
30. Shen, X. Y.; Tong, H.; Zhu, Z. H.; Wan, P.; Hu, J. M. *Mater. Lett.* **2007**, *61*, 629.
31. Montserrat, G. A.; Francisco, L. C.; Margarita, M. J. *Polym. Sci. Part B Polym. Phys.* **1997**, *35*, 2379.